

# CURRENT DEVELOPMENTS FOR INCREASING THE BEAM INTENSITIES OF THE RIKEN 18-GHz SUPERCONDUCTING ECR ION SOURCE

T. Nagatomo\*, Y. Kotaka†, V. Tzoganis‡, M. Kase, T. Nakagawa, O. Kamigaito  
 RIKEN Nishina Center, Saitama 351-0198, Japan  
 Y. Ohshiro, Center for Nuclear Study, Univ. of Tokyo, Saitama 351-0198, Japan

## Abstract

The RIKEN 18-GHz superconducting ECR ion source (18-GHz SC-ECRIS) and the RIKEN AVF cyclotron function as the light-ion injector at the RI Beam Factory (RIBF) as well as being used for low-energy nuclear physics experiments and additional RI production. We are currently trying to measure and improve the beam quality of the 18-GHz SC-ECRIS because the beam intensities are lower than those obtained from the other injector using the RIKEN Linear Accelerator (RILAC). In order to improve our understanding and to increase the beam intensities, we are developing the simulation of the low energy beam transportation and an online emittance meter based on the pepper-pot method. We have tested a prototype emittance meter and confirmed an analysis procedure to deduce the emittance from the measured data.

## INTRODUCTION

Since the RIKEN AVF cyclotron was constructed in 1989, it has been used as an injector for the RIKEN ring cyclotron (RRC). It has been used as stand-alone experiments related to low-energy nuclear physics and RI production. Since April 2009, the AVF injection mode started in the RIKEN RI Beam Factory (RIBF), where the cascaded chain of AVF, RRC, and Superconducting Ring Cyclotron (SRC) has provided light ion beams such as D,  $^{14}\text{N}$ , and  $^{18}\text{O}$  ions. The RIKEN 18-GHz superconducting ECR ion source (18 GHz SC-ECRIS) is one of three ion sources used for the AVF cyclotron as shown in Fig. 1. One of the current problems in the AVF injection mode is that the beam intensities are significantly lower than those obtained with the RIKEN Linear Accelerator as the injector (the RINAC injection mode), as show in Table 1. In order to increase the beam current of the AVF injection mode, a comprehensive understanding of the behavior of the ion beam not only around the extrac-

Table 1: Beam intensities achieved from SRC.

Beam	Energy / A (MeV)	Intensity (pnA)	Injector
$^{18}\text{O}$	230	400	AVF
$^{18}\text{O}$	250	200	AVF
$^{18}\text{O}$	345	1000	RILAC

\* nagatomo@riken.jp

† SHI Accelerator Service Ltd., Tokyo, Japan

‡ The University of Liverpool, Liverpool, United Kingdom

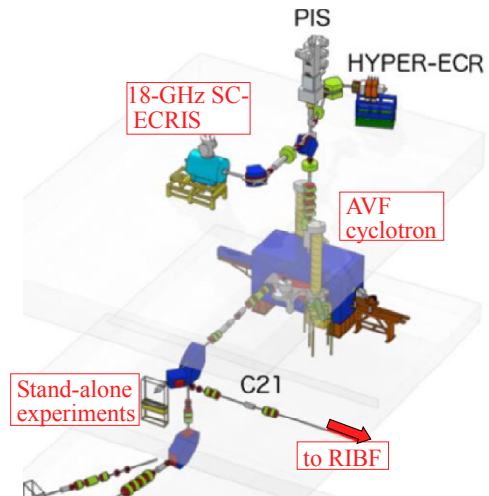


Figure 1: Schematic view of the RIBF injector apparatus with the 18-GHz SC-ECRIS.

tion area of the ion source but also for the low energy beam transport (LEBT) to the AVF cyclotron is necessary. To this end, we have started developing simulations to elucidate the ion trajectory through the LEBT and an online emittance monitoring system based on the pepper-pot method [1]. The current status of the 18-GHz SC-ECRIS is also discussed.

## APPARATUS

The 18-GHz SC-ECRIS is one of the ion source for the AVF cyclotron. At present, the 18-GHz SC-ECRIS mainly provides light-ion beams generated from gaseous elements, e.g.  $\text{D}^+$ ,  $^{12}\text{C}^{4+}$ ,  $^{18}\text{O}^{6+}$ ,  $^{40}\text{Ar}^{11+}$  ions and so on. The dimensions of the SC-ECRIS and LEBT are shown in Fig. 2. The specifications of the 18-GHz SC-ECRIS are given in Table 2. The length and diameter of the plasma chamber are 70 mm and 378 mm, respectively. The plasma chamber is encapsulated by a hexapole permanent magnet of which the magnetic field is  $\sim 1.1$  T at the surface. A set of superconducting solenoids is used to achieve the minimum- $B$  condition. A moveable biased disc with a diameter of 30 mm is installed, to which a negative voltage of a few hundred volts with respect to the plasma chamber can be applied to increase the multi-charged ion flux. A 750-W TWTA (XTRT-750DBS, Comtech Xicom Technology, Inc) is installed to generate the 18-GHz microwaves that induce the ECR heating. The multi-charged ions are extracted and accelerated towards a grounded extraction electrode by applying a high voltage,

ISBN 978-3-95450-158-8

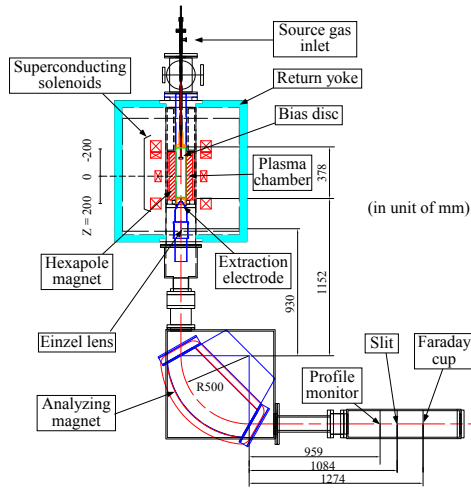


Figure 2: Schematic of the 18-GHz SC-ECRIS and LEBT leading to the AVF cyclotron.

typically 10 kV, to the plasma chamber. The extracted ion beam is passed through an Einzel lens installed just behind the extraction electrode, analyzed by the analyzing magnet of the LEBT and fed into the AVF cyclotron. The LEBT consists of an analyzing magnet and a diagnosis chamber in which a profile monitor, a set of horizontal and vertical slits and a Faraday cup are installed. At present, there is no device for measuring the beam emittance in the LEBT.

Table 2: Specifications of the 18-GHz SC-ECRIS.  $B_{||}$  is the longitudinal magnetic field along the axis of the ion source at the designed maximum current density of  $100 \text{ A/mm}^2$ .

18-GHz SC-ECRIS	
Superconducting material	Nb-Ti
Bore (room temperature)	220 mm
Radius of plasma chamber	70 mm
Length of plasma chamber	378 mm
Length of hexapole magnet	380 mm
$B_{  }$ ( $z = -200$ mm)	3.0 T
$B_{  }$ ( $z = 0$ mm)	0.6 T
$B_{  }$ ( $z = 200$ mm)	2.0 T
Frequency of the ECR microwave	18 GHz
Typical power of the ECR microwaves	500 W
Typical extraction voltage	10 kV
Analyzing magnet in LEBT	
Pole gap	80 mm
Radius of curvature $\rho$	500 mm
Bending angle	90 degrees
$B_{\text{max}}$	0.15 T
Edge angle	29.6 degrees

## DEVELOPMENTS

### Beam Transport simulation in LEBT

Simulating the beam transportation is an effective method of estimating the quality of the extracted beam from the ion source. An important point in the simulation is to use accurate electromagnetic field maps calculated with three-dimensional models to reduce errors. We employed OPERA-3D [2], an approach based on the finite element method, to calculate the mirror field generated by the superconducting solenoids and the hexapole magnet, the electric field generated by the extraction electrode and the Einzel lens, and the magnetic field produced by the analyzing magnet.

The strength of the mirror field around the end of the plasma chamber is related to the density of the plasma, which influences the envelope of the extracted beam. The estimated field map for the transverse magnetic field  $B_{\perp}$  at the end of the plasma chamber is shown in Fig. 3. In the future, we are planning to simulate a realistic beam transport with a initial condition in which the beam density is determined by the strength of the mirror field and evaluate the beam profile obtained using the emittance meter. On the other hand, the absolute value of the mirror field on the ion source axis is shown in Fig. 4. Fig. 4 shows that the Einzel lens is not placed at the optimum position because the mirror field is over 0.3 T at the lens center ( $z = 385$  mm).

The beam transportation is simulated through a Monte Carlo approach using the geant4 tool kit [3], taking the actual geometries of the beam line and the electromagnetic field maps into account. The space-charge effect is currently not included in the simulation. The simulation estimates the momentum dispersion at the slit position to be  $-22.05 \text{ mm}/\%$ . Two setups for the transportation of  $^{12}\text{C}^{5+}$  ions of 50 keV are shown in Fig. 5; the first is for parallel beams having the horizontal size of  $\pm 10$  mm and the second is for beams emitted from a point source with an angular spread of  $\pm 40$  mrad. In both cases, no voltage was applied to the Einzel lens. Comparing the figures shows that it is important to control the emission angle of the beam because the focus

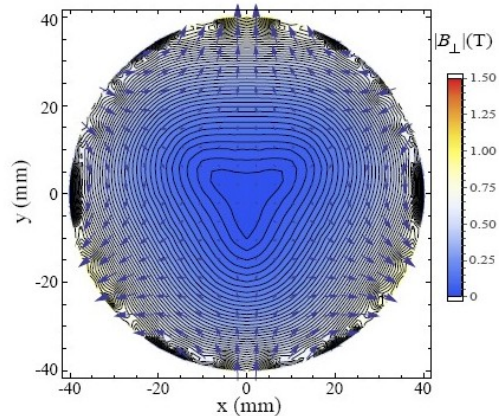


Figure 3: Estimated map of the transverse component of the mirror field at the end of the plasma chamber.

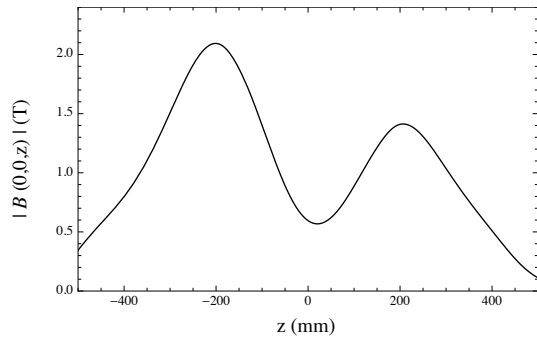


Figure 4: Absolute value of a typical mirror field along the ion source axis.

point of the tilted beam is shifted behind the focus of the parallel beam. With the simulation at this stage, we can now attempt to incorporate the space-charge effect. However, treating such collective effects consistently in event-by-event Monte Carlo simulations remains an open problem.

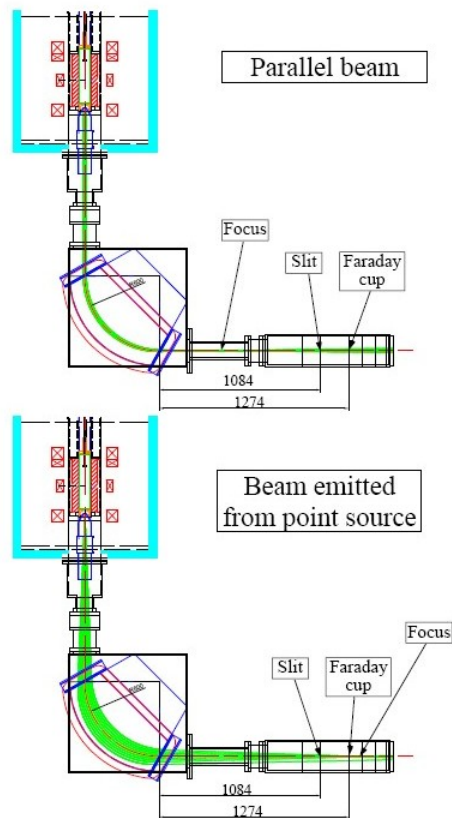


Figure 5: Setups for  $^{12}\text{C}^{5+}$  transportation. Top: parallel beam with the initial x position spread across  $\pm 10$  mm. Bottom: beam emitted from a point source over  $\pm 40$  mrad. The ion beam trajectories are shown as green lines.

### Emittance Meter

A prototype of a pepper-pot emittance meter [1] has been developed through a collaborative project between RIKEN and Center for Nuclear Study, the University of Tokyo (CNS) [4]. On the pepper-pot plate, there are 480 holes with the diameter of 0.357 mm at intervals of 2 mm aligned in a lattice structure. In the downstream (65 mm) of the pepper-pot plate, a fluorescent screen (a copper plate covered with KBr) is placed tilted at an angle of 45 degrees with respect to the beam direction. Its role is to produce images that are captured using a digital camera that is set perpendicular to the beam direction. On the fluorescence screen, crossed lines of 11 holes are drilled at a certain pitch to calibrate the length of the obtained image and to account for distortion of the image due to the tilt of the screen. In addition, the hole at the center of the pepper-pot plate was masked to indicate the center of the fluorescence image on the screen. As shown in Fig. 6, a fluorescence image induced by the 10-keV proton beam passing through the pepper-pot holes was successfully obtained. The proton beam was provided by another ECR ion source, Hyper-ECR in Fig. 1, which belongs to CNS. The beam intensity was  $95 \mu\text{A}$ .

In order to estimate the beam emittance, it is necessary to determine the correspondence between the beam spots on the screen and the holes on the pepper-pot plate. From the difference in transverse position between the beam spot and the corresponding pepper-pot hole, angles with respect to the beam direction were obtained as a function of the beam position. In addition, the brightness of the beam spot is proportional to the beamlet intensity in principle, meaning the beam emittance can be determined from only a single shot of the image. After the calibration and correction discussed above were applied to the obtained image, the image was transformed to fit the transverse coordinates of the beam frame, x, y and z, which correspond to the horizontal, vertical and beam axes, respectively. From the transformation, the beam image in the x-y plane is shown in Fig. 7. The beam image is separated into segments using the troughs in

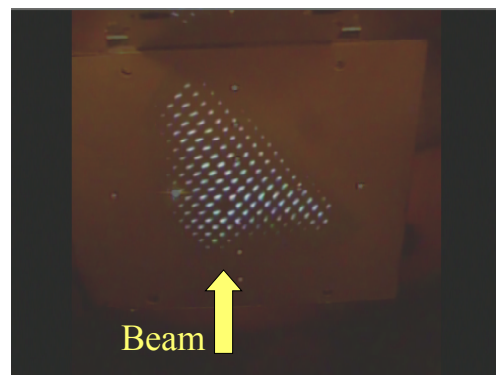


Figure 6: Image of the beam spots induced by the 10-keV protons passing through the pepper-pot plate, together with an image of the fluorescence screen with several holes used for calibration and correction.

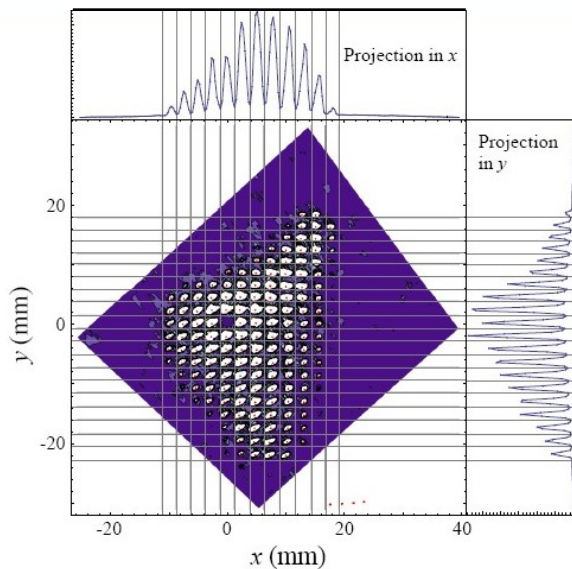


Figure 7: Contour plot showing the beam intensity, which is extracted from the pepper-pot image, transformed to transverse coordinates. The projections in the  $x$  (horizontal) and  $y$  (vertical) axes are also shown.

the  $x$  and  $y$  projections. By searching for a segment with smaller intensity that is surrounded by segments with higher intensities, the segment corresponding to the masked pepper-pot hole is identified on the fluorescent screen. Taking the masked position as a reference, we identified the correspondence between the pepper-pot holes and the beam spots. From the transverse position difference between these corresponding holes and spots, the beam emittance was obtained as shown in Fig. 8.

Although this is an offline analysis, the procedure described here was quickly and automatically executed; thus, we have confirmed that the algorithm works well. Further developments to incorporate the algorithm into the image acquisition system using LabView (National Instruments Co.) are in progress to establish an online emittance monitor.

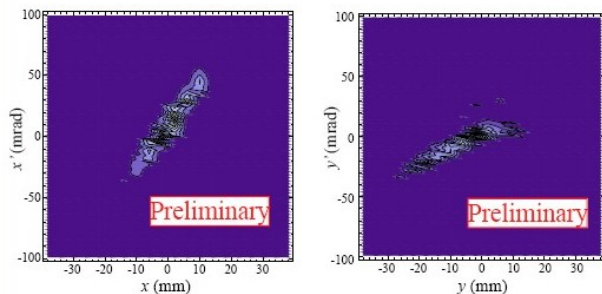


Figure 8: Beam emittance obtained from the pepper-pot image in Fig. 6. The left figure shows the emittance in horizontal phase space and the right in vertical phase space.

## SUMMARY AND FUTURE PROSPECTS

A combination of the RIKEN 18-GHz SC-ECRIS and AVF cyclotron is used as the injector for the RIKEN RIBF, providing light-ion beams such as D,  $^{14}\text{N}$  and  $^{18}\text{O}$  ions. However, at present, the beam intensity is lower than that provided with the RILAC injection mode. In order to increase the beam intensity, a comprehensive understanding of the properties of the 18-GHz SC-ECRIS and the subsequent LEBT is required. Using geant4, Monte Carlo simulations of the LEBT were performed. We employed OPERA-3D, which is based on the finite element method, to calculate an electromagnetic field map using an accurate 3D model of the magnets and electrodes. The current transport simulation does not account for the space-charge effect. In order to investigate the properties of the beam from the 18-GHz SC-ECRIS, development of a pepper-pot emittance meter is in progress. Using a prototype device, we obtained an image of the beam spots with a 10-keV proton beam with an intensity of  $90\ \mu\text{A}$ . An algorithm to automatically determine the correspondence between the pepper-pot holes and the beam spots on the fluorescent screen was confirmed and the beam emittance was obtained. The incorporation of this algorithm into the data acquisition system is also in progress in order to create an online emittance meter.

As the intensity of a highly charged ion beam increases just after extraction from the ion source, the space-charge effect considerably degrades the beam quality due to its low energy and high charge density. In the future, we are planning to investigate the relationship between the beam quality and the beam intensity with the online emittance meter and simulations in order to improve the beam quality.

## REFERENCES

- [1] C.C. Cutler and J.A. Salom, Proc. IRE 43, 299 (1955), C.C. Cutler and M.E. Hins, Proc. IRE 43, 307 (1955).
- [2] "OPERA-3D" is a code suite for electromagnetic field calculations developed by Cobham PLC <http://operafea.com>
- [3] S. Agostinelli et al., Nucl. Inst. and Meth. A 506, 250 (2003), J. Allison et al., IEEE Trans. on Nucl. Sci. 53, No. 1, 270 (2006)
- [4] Y. Kotaka et al., to be published in the Proceedings of the 11th Annual Meeting of the Particle Accelerator Society of Japan (2014).